Journal Pre-proof

Fine air pollution particles trapped by street tree barks: In situ magnetic biomonitoring

Marcos A.E. Chaparro, Mauro A.E. Chaparro, Ana G. Castañeda-Miranda, Débora C. Marié, José D. Gargiulo, Juan M. Lavornia, Marcela Natal, Harald N. Böhnel

PII: S0269-7491(20)33287-5

DOI: https://doi.org/10.1016/j.envpol.2020.115229

Reference: ENPO 115229

To appear in: *Environmental Pollution*

Received Date: 29 April 2020

Revised Date: 27 June 2020

Accepted Date: 9 July 2020

CRediT author statement

Marcos Chaparro: Conceptualization, Supervision, Writing- Original draft preparation, Funding acquisition. **Mauro Chaparro**: Investigation, Formal analysis, Software, Visualization. **Ana Castañeda-Miranda**: Investigation, Methodology. **Débora Marié**: Investigation. **José Gargiulo**: Investigation. **Juan Lavornia**: Investigation, Methodology. **Marcela Natal**: Investigation. **Harald Böhnel**: Writing-Reviewing and Editing, Funding acquisition.

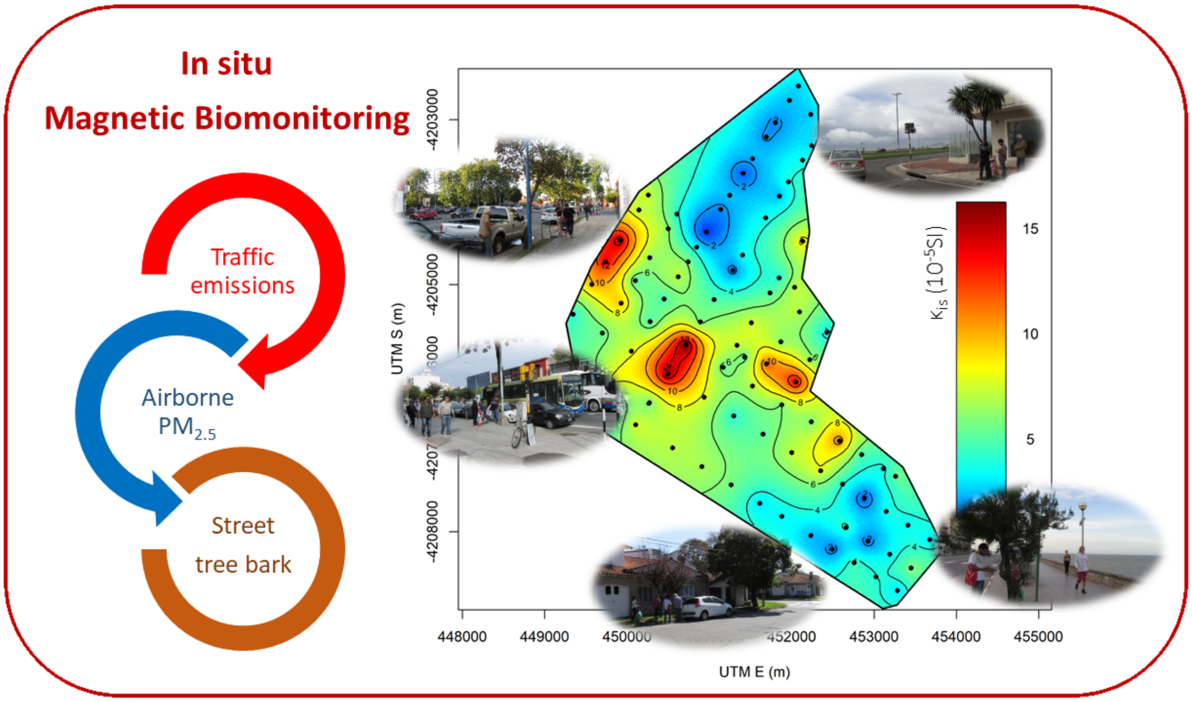
In situ
Magnetic Biomonitoring
Traffic emissions
Airborne PM2.5
Street tree bark
UTM S (m)
-4203000
-4205000
-4208000
UTM E (m)
448000
449000
450000
452000
453000
454000
455000
Kis (10-5SI)
15
10
5

Fine air pollution particles trapped by street tree barks: in situ magnetic biomonitoring

Marcos A. E. Chaparro[1,*]; Mauro A. E. Chaparro[2]; Ana G. Castañeda-Miranda[1]; Débora C. Marié[1]; José D. Gargiulo[1]; Juan M. Lavornia[3]; Marcela Natal[2]; Harald N. Böhnel[4]

1 Centro de Investigaciones en Física e Ingeniería del Centro de la Provincia de Buenos Aires (CIFICEN, CONICET-UNCPBA), Pinto 399, 7000 Tandil, Argentina.

2 Centro Marplatense de Investigaciones Matemáticas (CEMIM-UNMDP-CONICET), Diagonal J. B. Alberdi 2695, Mar del Plata, Argentina.

3 Instituto de Ciencias Polares, Ambiente y Recursos Naturales (ICPA), Universidad Nacional de Tierra del Fuego (UNTDF), Fuegia Basket 251, 9410, Ushuaia, Argentina.

4 Centro de Geociencias (CGeo), Universidad Nacional Autónoma de México (UNAM), Boulevard Juriquilla No. 3001, 76230 Querétaro, México.

[*]Name and contact detail of the corresponding author: Marcos A.E. Chaparro. CIFICEN, CONICET-UNCPBA, Pinto 399, B7000GHG Tandil, Argentina. Phone: +54 249 4385661. E-mail: chapator@exa.unicen.edu.ar. ORCID ID: 0000-0003-2832-2151. Scopus ID: 26425631300.

Abstract

Particulate air pollution in cities comprises a variety of harmful compounds, including fine iron rich particles, which can persist in the air for long time, increasing the adverse exposure of humans and living things to them. We studied street tree (among other species, *Cordyline australis*, *Fraxinus excelsior* and *F. pensylvanica*) barks as biological collectors of these ubiquitous airborne particles in cities. Properties were determined by the environmental magnetism method, inductively coupled plasma optical emission spectrometry and scanning electron microscopy, and analyzed by geostatistical methods. Trapped particles are characterized as low-coercivity (mean±s.d. value of remanent coercivity $H_{cr} = 37.0 \pm 2.4$ mT) magnetite minerals produced by a common pollution source identified as traffic derived emissions. Most of these Fe rich particles are inhalable ($PM_{2.5}$), as determined by the anhysteretic ratio χ_{ARM}/χ (0.1 – 1 µm) and scanning electron microscopy (< 1 µm), and host a variety of potentially toxic elements (Cr, Mo, Ni, and V). Contents of magnetic particles vary in the study area as observed by magnetic proxies for pollution, mass specific magnetic susceptibility χ ($18.4 - 218 \times 10^{-8}$ m^3 kg^{-1}) and in situ magnetic susceptibility κ_{is} ($0.2 - 20.2 \times 10^{-5}$ SI). The last parameter allows us doing in situ magnetic biomonitoring, being convenient because of species preservation, measurement time, and fast data processing for producing prediction maps of magnetic particle pollution.

Keywords: air pollution; biomonitor; environmental magnetism; geostatistical method; magnetic proxy; magnetite

***Capsule**: "magnetic biomonitoring using street tree bark is convenient because of measurement time and fast data processing for producing maps of particle air pollution"*

1. Introduction

Air pollution in urban areas is a serious human problem and hence a subject of increasing global concern. Although clear signals of this problem are distinctly evident in large and megacities (Karagulian et al., 2015; Gargiulo et al., 2016), smaller cities, towns, and even small human settlements in remote Antarctica (Chaparro et al., 2007) experience pollution signals as well. This is true because of a critical part of gases and particulate matter (PM) spreading over cities are emitted by mobile sources such as motor vehicles. Such PM emissions come from combustion engines, general metal corrosion, and mechanical abrasion of road material, tires and brake systems (Palmgren et al., 2003; Chan and Stachowiak, 2004; Chaparro et al., 2010; Gietl et al., 2010). These emissions include inhalable iron oxides (ferro- and ferrimagnetic materials) and potentially toxic elements (PTE), among other potentially harmful compounds. And more important, they comprise micro- to nanoparticles that can reach vital human organs –lungs, heart and brain– via the respiratory, blood circulation and olfactory systems (Maher et al., 2016; Calderón-Garcidueñas et al., 2019). Therefore, humans and other living organism present in every settlement on the earth faces the adverse effect of different anthropogenic pollutant loads.

Air quality, both indoors and outdoors, is closely related to morbidity and mortality from respiratory, cardiovascular and neurodegenerative diseases (Han and Naeher, 2006; Pope et al., 2002; Knox, 2006; Maher, 2019). Thus, there is a necessity of monitoring methodologies for airborne pollutants with adverse effects on human health. Among them, magnetic biomonitoring offers a simple, fast and cost-reduced alternative to assess the spatial and temporal patterns of contaminants. This technique was recently developed, and proposes the use of the environmental magnetism method and biological collectors, such as, lichen spp. (Chaparro et al. 2013, Marié et al., 2016; Paoli et al., 2017; Winkler et al. 2019), moss spp. (Fabian et al., 2011; Vuković et al., 2015; Salo et al., 2016), *Tillandsia* spp. (Castañeda-Miranda et al., 2016, Mejía-Echeverry et al., 2018), tree leaves (Moreno et al., 2003; Lehndorff et al., 2006; McIntosh et al., 2007; Sagnotti et al., 2009; Rai, 2013), tree ring cores and tree barks (Huhn et al., 1995; Kletetschka et al., 2003; Zhang et al., 2008; Brignole et al., 2018).

Most of these studies have been carried out using native species collection; however, recent magnetic biomonitoring studies have proved the advantage of species transplants (Salo and Mäkinen, 2019; Castañeda-Miranda et al., 2020; Winkler et al., 2020) for hotspots and specific study areas, as well as over controlled exposure periods. The usefulness of species transplantation methodology is the ability to control initial exposure conditions and time periods for sampling, measure magnetic properties (concentration, mineralogy, and grain size) over time, and choose sites of concern for purposes of temporal monitoring or control of airborne magnetic PM emissions (Marié et al., 2019). On the other hand, Marié et al. (2018) proposed the first methodology of "in situ magnetic biomonitoring" by measurements of in situ magnetic susceptibility κ_{is} on lichens, which preserves species in its habitat and allows doing magnetic measurements over different periods of time. A detailed data collection over time was possible through this novel methodology, by collection and analysis of a total of ~8300 measurements of κ_{is} over 60 measurement surveys.

This study proposes the use of street trees in cities for assessing airborne particulate contamination. Trapped vehicle derived pollutants (magnetic particles and PTE) were studied by the environmental magnetism method, inductively coupled plasma optical emission spectrometry (ICP-OES), and scanning electron microscopy and X-ray energy dispersive spectroscopy (SEM-EDS). After determining magnetic properties and elemental composition of trapped particles, their relationship was studied by multivariate analysis. An in situ magnetic biomonitoring was carried out on tree barks, producing κ_{is} measurements. Such data were analyzed by geostatistical techniques, from which prediction maps of magnetic susceptibility were obtained.

2 Sampling and laboratory methods

Detailed information of this section can be found in Supplementary Material.

2.1. Study area and sampling

Mar del Plata is one of the largest cities in the Buenos Aires province in Argentina, located at latitude 38° 00’ S and longitude 57° 33’ W in the SE of the province (Fig. 1). A total of 560,000 vehicles, i.e.: 400,000 motor vehicles (cars and public buses) and 160,000 motorcycles, from the stable population were informed in 2015 (I Informe Anual de Mar del Plata, 2015). An initial sampling area of about 7.4 km^2 (54 sampling sites) was studied in April 2016, which was enlarged to 10.7 km^2 (96 sampling sites) for the second survey in March 2017 (Fig. 1). The in situ magnetic biomonitoring was carried out during the second sampling survey. Within the sampling area, a sampling grid of 0.2 km × 0.3 km was used. Different available tree species inside the study area were censed; nine street tree species were selected, identified and classified by gender and family. The ages of the sampled trees were estimated by the method proposed by the International Society of Arboriculture (ISA), which is based on the tree diameter at breast height (DBH) and the average growth rate for each species.

2.2. Magnetic measurements

Dried tree bark material (0.4 – 1.2 g) was firmly pressed and placed into plastic containers of 2.3 cm^3 for routine magnetic measurements. Tree bark samples were labeled as MC samples. Mass specific magnetic susceptibility (χ), percentage frequency-dependent susceptibility ($\chi_{fd}\% = 100\ (\chi_{0.47kHz} - \chi_{4.7kHz}) / \chi_{0.47kHz}$), mass specific anhysteretic susceptibility (χ_{ARM}), anhysteretic ratio χ_{ARM}/χ, saturation of isothermal remanent magnetization (SIRM = IRM_{2470mT}), remanent coercivity (H_{cr}), and S-ratio ($S_{-300} = -IRM_{-300mT}$ / SIRM) were calculated. The temperature dependence of high-field magnetization was carried out using a laboratory-made horizontal magnetic translation balance (Escalante and Böhnel, 2011). Measurements of κ_{is} were done at the high resolution range (0.1×10^{-5} SI). κ_{is} values were corrected for drift through a 3 measurement protocol (two air and one sample readings). At each street tree, five corrected values of κ_{is} were averaged obtaining a representative measurement.

2.3. Chemical analysis and microscopy observations

Ba, Co, Cr, Cu, Fe, Mo, Ni, Pb, Sb, Sn, V, and Zn were determined in 27 samples by inductively coupled plasma optical emission spectrometry. The pollution load index (PLI) defined by Tomlinson et al. (1980), is a composite index based on the mentioned PTE. It was calculated using equation (1),

$$PLI = \sqrt[n]{\prod_{i=1}^{n} \frac{C_i}{C_{base,i}}} \qquad (1)$$

where C_i is the concentration of each PTE, and $C_{base,i}$ is the baseline value for each element, obtained from minimum values. Tree barks were observed and examined by scanning electron microscopy using a Phillips microscope model XL30. This microscope also allowed to analyze the elemental composition of single particles by X-ray energy dispersive spectroscopy with an EDAX model DX4 (detection limit 0.5%).

2.4. Statistical analysis

The statistical and multivariate analyses were performed using R (version 3.4.0, 2017). The Ordinary Kriging method was used to build prediction maps of the most relevant magnetic parameter.

3. Results

3.1. Street tree species

41 tree species are found in Mar del Plata. The city council has recommended 34 street tree species for urban, suburban and coastal zones since 2018. A list of such recommended and excluded species are detailed at EMSUR (2018). Among the 54 sampling sites, 11 species belonging to 9 families –Asparagaceae, Bignonacea, Fabaceae, Malvaceae, Oleaceae, Pinaceae, Roseceae, Salicaceae, and Sapindaceae– were identified for this magnetic

biomonitoring. As observed in Figure 2, *Cordyline australis* (G.Forst.) Endl., and *Fraxinus excelsior* L., *F. pensylvanica* L. are the most abundant species for this study.

According to the age estimation using the DBH and the average growth rate, ages of sampled street trees are between 21 and 138 years (Table S1, Supplementary Material). Therefore, all sampled trees in this study exceed the monthly/annual exposure to particle pollution. Studied samples of these species are represented in the following order, *F. excelsior* and *F. pensylvanica* (34.6% of samples), *C. australis* (32.7%), *Acer negundo* and *A. pseudoplatanus* (5.8%), *Catalpa speciosa* (5.8%), *Prunus cerasifera* (5.8%), *Albizia julibrissin* (5.8%), *Cedrus deodora* (3.8%), *Tilia moltkei* (3.8%), and *Populus nigra* (1.9%).

3.2. Airborne magnetic particles

Measurements of isothermal remanent magnetization acquisition evidence that samples reached 95 – 97% of their saturation at 200 mT. Although S-ratio ranges from 0.80 to 1, most of values are between 0.90 – 0.98, indicating the dominance of ferrimagnetic minerals with relatively low coercivity. Values of remanent coercivity ranges from 27.0 to 40.1 mT, with mean ± s.d. value of H_{cr} = 37.0 ± 2.4 mT (Table 1).

Thermomagnetic studies (M-T measurements) of seven MC-samples are shown in Figure 3a, where Curie temperatures (T_c) were calculated from the second derivative of M(T). Heating runs show a similar magnetic behavior among different MC sites, which is indicative of a common production source for trapped magnetic particles on street tree barks. This fact is also observed in Figure 3b through the relationship between SIRM and χ ($R = 0.86$, $p < 0.01$). A main ferrimagnetic phase with T_c = 553 – 561 °C was determined, according to literature (Dunlop and Özdemir, 1997; Liu et al., 2012), it corresponds to magnetite-like mineral. In addition, a minor high-coercivity phase with T_c = 626 – 670 °C was also determined. Such minor magnetic phase may be associated to traffic derived emission (diesel exhausts and/or asphalt debris as reported by Marié et al., 2010), mixed traffic and industrial emission (Castañeda-Miranda et al., 2016; Marié et al., 2016) or to soil particles. Differences between heating and cooling curves in the range RT – 720 °C evidence differences in magnetic behavior between samples MC-1.4 and MC-1.3/3.4/3.8/6.2/8.1/8.2. Magnetization increased between 38 – 88% for cooling runs at RT as consequence of a neo-formation of magnetite mineral.

Measurements of magnetic concentration dependent parameters χ and SIRM are represented in Figure 3b, both parameters are recognized magnetic proxies for pollution. The magnetic proxy χ is the most used parameter because of being determined with high sensitivity, fast laboratory processing, and susceptibility meter is of relatively low cost. Magnetic susceptibility is roughly proportional to concentration of paramagnetic and ferromagnetic minerals, but parameter SIRM is only sensitive to ferromagnetic minerals. As summarized in Table 1, mean ± s.d. values of mentioned parameters are relatively high for MC samples, χ = 82.2 ± 40.0 $\times 10^{-8}$ m^3 kg^{-1}, SIRM = 9.3 ± 4.3 $\times 10^{-3}$ A m^2 kg^{-1}, being four-fold higher than their corresponding minimum values. According to Dunlop and Özdemir (1997), χ_{ARM} is a concentration and grain size dependent magnetic parameter. Mean ± s.d. value of this parameter is 287 ± 139 $\times 10^{-8}$ m^3 kg^{-1} (three-fold its minimum value).

Anhysteretic ratios χ_{ARM}/χ and ARM/SIRM are magnetic grain size dependent parameters that have mean ± s.d. values of 4.0 ± 2.4 and 0.03 ± 0.01, respectively (Table 1). Both ratios are normalized with concentration dependent parameters for cancelling the effect of magnetic concentration, and enhance the signal due to variations in grain size (Liu et al., 2012). χ_{ARM}/χ is a sensitive grain size indicator of magnetite, where values of $\chi_{ARM}/\chi > 2.4$, and > 5.7 are indicative of the presence of very small magnetite particles (< 1 μm, and 0.1 μm, respectively, estimation based on King et al., 1982). Airborne magnetic particles in this study area are emitted mainly by mobile sources such as cars, motorcycles and public buses. Traffic emission is one of the main adverse pollution activity in Mar del Plata, where a high number of motor vehicles (560,000) from the stable population can increase by 25% or more by tourism activity (I Informe Anual de Mar del Plata, 2015). Percentage frequency-dependent susceptibility (mean ± s.d. value of $\chi_{fd}\% = 4.1 \pm 3.8\%$) indicates the presence of superparamagnetic (SP) particles (ultrafine ferrimagnetic particles <0.03 μm) and other ones. These values belong to the range $\chi_{fd}\% = 2 - 10\%$, corresponding to an admixture between SP and coarser particles (Walden et al., 1999). Another size related ratio SIRM/χ, which correlates with χ_{ARM}/χ ($R = 0.78$, $p < 0.01$), has mean ± s.d. value of 13.1 ± 8.4 kA/m. High values indicate fine magnetic particles.

Some of these fine magnetic particles trapped on the surface of tree barks can be observed by SEM microscopy. As appreciated in Figure 4, most of particles are < 1 μm corresponding to the dangerous category of $PM_{2.5}$. Fe-rich irregular particles (Fig. 4a, 4b, 4d, and 4e) and spherules (Fig. 4c, 4e, and 4f) are observed, their composition by EDS shows the co-existence of Fe with Al, Si, Ca, Ti, Ni, Cr, and Ce.

As reported in literature, these Fe-rich particles emitted by motor vehicles can host PTE into their crystalline structure or onto their surface (adsorption). In Table 1, mean values of Ba (101 mg kg^{-1}), Co (0.9 mg kg^{-1}), Cr (4.8 mg kg^{-1}), Cu (48 mg kg^{-1}), Fe (3160 mg kg^{-1}), Mo (1.07 mg kg^{-1}), Ni (2.9 mg kg^{-1}), Pb (32.4 mg kg^{-1}), Sb (2.5 mg kg^{-1}), Sn (1.4 mg kg^{-1}), V (5.4 mg kg^{-1}), and Zn (1650 mg kg^{-1}) are listed. Such mean values, except Co, surpass two-fold to five-fold their corresponding minimum values, which evidences different pollution loads regarding specific areas within Mar del Plata.

4. Discussion

4.1. Magnetic carriers and potentially toxic elements

Airborne magnetic particles collected by these street barks are characterized as low-coercivity magnetite minerals. Thermomagnetic M(T) and IRM acquisition curves showed similar patterns between MC samples, which evidence a common pollution source, that is, mentioned traffic derived particles. Mineralogy dependent magnetic parameters (T_c, S-ratio, and H_{cr}) varied in a narrow range (T_c = 553 – 561 °C, and mean ± s.d. of H_{cr} = 37.0 ± 2.4 mT, Table 1), corresponding to magnetite mineral. These results agree well with data from vehicle derived studies reported by Chaparro et al. (2010): T_c = 580 °C and H_{cr} = 33.1 ± 8.6 mT for diesel soot, T_c = 580 °C and H_{cr} = 31.0 ± 5.4 mT for gasoline soot. Moreover, they are also in agreement with other magnetic biomonitoring studies carried out in cities from Buenos Aires province, using a lichen sp.: T_c = 553 – 575 °C and H_{cr} = 34.2 ± 2.5 mT for Tandil (Marié et al., 2016); H_{cr} = 38.2 ± 1.3 mT for Mar del Plata (Gómez et al., 2018); and a *Tillandsia* sp.: H_{cr} = 36.3 ± 1.6 mT for La Plata (Castañeda-Miranda et al., 2018).

The composite PLI index shows values above 1, which is a reference value for minimum contamination by PTE. Results of this index (calculated using Eq. 1 and PTE data, Table 1) give an assessment of the overall pollution status for each MC sample. Mean ± s.d. value of PLI is 3.3 ± 1.3, such values exceed three-fold the contents of elements for a reference (unpolluted) environment. The multivariate analysis show that these magnetic particles host potentially toxic elements. Among magnetic parameters, concentration dependent ones χ and SIRM are correlated with Fe, Cr, Mo, Ni, V, and the pollution index PLI. The best relationships are observed for χ with Cr ($R = 0.64$, $p < 0.01$); Fe ($R = 0.61$, $p < 0.01$); Mo, Ni, V and PLI ($R = 0.51 – 0.52$, $p < 0.01$); and Ba ($R = 0.45$, $p < 0.05$). SIRM correlates significantly with Ba, Cr, Fe, Mo and Ni ($R = 0.41 – 0.45$, $p < 0.05$). On the other hand, the anhysteretic ratio χ_{ARM}/χ correlates inversely with Cu and Zn ($R = -0.41$, $p < 0.05$).

Most of PTE, PLI, χ and SIRM surpass up to five-fold their corresponding minimum values, which is indicative of the atmospheric pollution contribution within the city. Ba, Cr, Mo, Ni, Cu and Zn have been reported in other magnetic monitoring of traffic emissions (Weckwerth, 2001; Lin et al., 2005; Maher et al., 2008; Sagnotti et al., 2009). According to Lim et al. (2007), Ba, Cr, Fe, Cu and Zn are present in fuels and lubricating oils as additives. Such PTE and other ones are emitted by mobile sources, that is after combustion (Ba, Zn, Ni, Fe, Cr, and Cu, Lu et al., 2005; Marié et al., 2010), and by general corrosion, engine and brake abrasion (Fe, Al, Si, Ca, Mo, Ba, Zn and Cu, Sanders et al., 2003; Chan and Stachowiak, 2004).

4.2. Potentially dangerous particles

These Fe-rich particles are not only harmful by hosting PTE, but also because of their ultrafine/fine size as observed by SEM- EDS (Fig. 4) of often < 1 µm. They are potential dangerous particles that are inhalable, and therefore, adverse for humans and other living organisms. Size distribution of all samples consists of submicron and micron magnetite particles (Fig. 5).

MC grain size data is represented in Figure 5a with other available data from vehicle emissions (Marié et al., 2010) and magnetic biomonitoring studies carried in cities from Buenos Aires province, in particular, using lichen sp. in Tandil (Marié et al., 2016) and Mar del Plata (Gómez, 2019), and using *Tillandsia* sp. in La Plata (Castañeda-Miranda et al., 2018). Most of them fall in the range < 0.1 – 1 µm and correspond to the category $PM_{2.5}$. Comparison of MC sizes is in agreement with ranges obtained for mentioned biomonitoring studies. As appreciate in Figure 5b, the mean value of size (and anhysteretic ratio χ_{ARM}/χ) for this tree bark data is slightly lower than values recorded by lichen sp. but higher than *Tillandsia* sp. Although a complex composite of vehicle derived particles is expected in these barks, contribution of exhausts, brake systems and asphalt has to be different (because of their sizes) to reach 1.5 m above the ground. Smaller particles of about 1 µm emitted by combustion of diesel and gasoline (mean χ_{ARM}/χ for gasoline/diesel PM is slightly lower than for MC samples) seem to be preferred and more probable trapped (and preserved) in this case than larger brake wear and asphalt debris (mean sizes of about 5 µm, Marié et al., 2010). This fact seems not to be related to the studied biomonitor (tree bark) itself because similar particle sizes were also observed in lichen species in this city. The partial loss of larger particles possibly of brake wear provenance may be explained by the role of rain, i.e. washing off and redistribution of such large particles, in exposed surfaces as well.

4.3. Particulate pollution: zones with high magnetic concentration

Dry and wet deposition of particles in the tree bark take place via direct incorporation or via the stem flow. Root uptake is another possible pathway from soils; however, magnetic particles (iron oxides) are not root-absorbed because they are insoluble in soil solutions (Huhn et al., 1995). Contents of airborne magnetic particles captured by street trees may vary within the study area by multiple factors, such as traffic volume, buildings, open coastal areas, commercial, recreational and residential areas, population density, etc. Although airborne particles are collected by different tree bark species, their collection represent similar time exposure over periods of months/years. As discussed by Catinon et al. (2008, 2011), airborne particles are deposited on the outer part of the tree bark, and then part of them are incorporated into the bark tissues. With time, some of these tree bark suber-included particles seem to undergo reductive dissolution into the deeper suber layers. Thus, tree bark surface-deposited and some suber-incorporated magnetic particles are expected to contribute to the magnetic signal in tree barks. Cross sections of some twigs studied by Flanders (1994) showed that magnetization of the core was almost two orders of magnitude below that of the surface. In *Salix matsudana* tree ring cores, Zhang et al. (2008) observed that magnetic particles (emitted by a Fe-smelting factory) were intercepted and collected by tree bark and then entered into tree xylem tissues during the growing season to become finally enclosed into the tree ring by lignification. Vezzola et al. (2017) observed a partial fragmentation of magnetite particles incorporated (encapsulated) into the bark, suggesting that plant physiological processes may dissolve or disintegrate such magnetite particles hosted in the inner part of barks. In addition, they found very low values of magnetic susceptibility (being frequently diamagnetic) and SIRM in inner bark (from inner layers) samples and close to values measured at a control site. Inter-species comparison using χ and κ_{is} values were studied here for the most representative species. Results from Kruskal-Wallis test show no significant differences ($p > 0.12$) between species through magnetic concentration dependent parameters (Table S2, Supplementary Material). Therefore, trapped magnetic particles are independent of the most representative species *F. excelsior* and *F. pensylvanica* (35% of samples), and *C. australis* (33%).

Magnetic proxies for pollution, χ and SIRM (Fig. 3b), accounted for the magnetic concentration variation recorded in tree barks (e.g.: $\chi = 82.2 \pm 40.0 \times 10^{-8}$ m^3 kg^{-1}), which is comparable to results obtained in other magnetic biomonitoring studies using lichen sp. in Tandil ($\chi = 105 \pm 94 \times 10^{-8}$ m^3 kg^{-1}, Marié et al., 2016) and Mar del Plata ($\chi = 119 \pm 38 \times 10^{-8}$ m^3 kg^{-1}, Gómez, 2018). On the other hand, similar results of magnetic concentration dependent parameters between tree barks and native lichen spp. for an industrial study area was reported by Paoli et al. (2017). Although surface capture of magnetic particles seems comparable between some tree barks and lichen species, there is a clear difference with tree leaves which may be related to their surface features (roughness, protective cuticle, etc.). In terms of surface magnetization (magnetization per unit area), Flanders (1994) found relative magnitudes of surface magnetization for green leaves, brown leaves, and barks are 1, 2.5, and 200, respectively.

Measurements of χ for two surveys over 2016 and 2017 were processed and are represented in Figure 6a and 6b. Prediction maps for both surveys were obtained using variogram functions of exponential type and by the spatial interpolation method, Ordinary Kriging. In general, lower values of χ are observed for 2017 survey than for 2016 one, may be due to the influence of rainier periods over 2017. Such fact is supported by meteorological data provided by the National Meteorological Service. Rainfall data during both campaigns is represented in Figure S1 (Supplementary Material), and as observed, recorded rainfall was higher for 2017 survey (47.6 mm) than for 2016 survey (21.6 mm). After moderate to intense rainy periods, a partial decrease of magnetic susceptibility is expected in lichens according to Marié et al. (2018). They highlighted that such decrease is indicative of two possibly inter-related pollutant dependent processes. The first one is related to a superficial "washing" of trapped particles on lichen's thallus and the second one to a reduction of dispersed airborne PM by wet deposition. A similar reduction of magnetic PM content by rainfall on tree leaves was also reported by Matzka and Maher (1999) and Castañeda-Miranda et al. (2020). Although decrease of χ over time is observed, about five main zones with high magnetic concentration are distinguished in 2016 survey ($\chi > 80 \times 10^{-8}$ m^3 kg^{-1}) and 2017 survey ($\chi > 70 \times 10^{-8}$ m^3 kg^{-1}). Such zones correspond to downtown Mar del Plata and main access to the city such as Pedro Luro Ave., Colón Ave., and Independencia Ave.

On the other hand, measurements of in situ magnetic susceptibility for biomonitoring are more convenient than laboratory measurements of χ because of execution time, preservation of biomonitors, and collection of κ_{is} data over different periods of time as proposed by Marié et al. (2018). After doing these rapid measurements and a fast-processing data procedure, prediction maps for 2017 survey (Fig. 7a) were obtained using mentioned variogram functions and Ordinary Kriging. Because of particles may be deposited unevenly on the tree bark surface and/or within inner suber layers, differences between laboratory (χ) and in situ (κ_{is}) magnetic susceptibility may arise from the integration volume where magnetic signal is measured (bark sample and bark surface, respectively) by sensors.

High values of in situ magnetic susceptibility ($\kappa_{is} > 8 \times 10^{-5}$ SI) allow identifying four main pollution zones within the study area. Such zones involve the highest population density (10,800 – 39,000 people per km^2) and the above mentioned avenues (Pedro Luro Ave., Colón Ave., Juan H. Jara Ave. and Independencia Ave., Fig. 1) where recorded traffic is the highest, between 19 – 64 veh min^{-1}, Fig. 7b). On the contrary, low values of κ_{is} ($< 4 \times 10^{-5}$ SI) defined two less pollution impacted zones located at NW and SE part (Fig. 7a). Both of these zones comprise residential areas (low population density of 3,000 – 6,000 people per km^2) with higher street tree density and lower transit (between 4 – 14 veh min^{-1}) than downtown.

5. Conclusion

Fe rich particles emitted by traffic pollution are collected from different street tree species, being *C. australis*, *F. excelsior* and *F. pensylvanica* the most abundant species for this study. Such particles are trapped in their tissue barks and are characterized by a low-coercivity phase of magnetite in agreement with traffic derived particles reported in literature.

These iron rich particles host a variety of dangerous elements such as Ba, Cr, Cu, Mo, Ni, Pb, Sb, Sn, V, Zn, Al, Si, Ca, Ti, and Ce. Some of these, as well as the pollution index PLI, surpass up to 5-fold their minimum values, which evidences the pollution influence. Another important result to be highlighted is that these particles fall in the size range of < 0.1 – 1 µm. These ultrafine/fine particles are inhalable and may reach deep into the lungs. Exposure to this $PM_{2.5}$ is associated with adverse effects on humans and other living things. Zones with high magnetic $PM_{2.5}$ concentrations were identified through prediction maps of χ and κ_{is}. Comparison between 2016 and 2017 surveys indicates a decrease of χ over time due to an increase of rainfall. In situ magnetic biomonitoring is a novel, rapid and convenient methodology for assessing particulate pollution by measurements of magnetic susceptibility and biomonitors. Such biomonitors (tree barks) have a low magnetic signal (due to their diamagnetic matrix) that may be enhanced by collecting minute amounts of ferrimagnetic vehicle derived particles. This fact, as well as availability and necessity of trees for multiple functions in cities, allows us the use of street tree barks as an efficient option for particulate biomonitoring in many cities around the world.

Conflict of interest

There is no conflict of interest.

Acknowledgements

The authors thanks to UNCPBA, CONICET and UNAM for their financial support. This contribution was supported by Agencia Nacional de Promoción Científica y Tecnológica

Project PICT-2013-1274 and the Bilateral CONICET/CONACYT Project No. 207149 (Harald Böhnel) and Res. 1001/14 - 5131/15 (Marcos Chaparro). The authors thank to the Editor and both anonymous reviewers whose comments greatly improved this manuscript. The authors also thank to, Ing. J. Escalante and Dr. Marina Vega (Centro de Geociencias, UNAM, México), and Michael Paarlberg for their help.

References

Brignole, D., Drava, G., Minganti, V., Giordani, P., Samson, R., Vieira, J., Pinho, P., Branquinho, C., 2018. Chemical and magnetic analyses on tree bark as an effective tool for biomonitoring: A case study in Lisbon (Portugal). Chemosphere 195, 508-514. https://doi.org/10.1016/j.chemosphere.2017.12.107.

Calderón-Garcidueñas, L., González-Maciel, A., Mukherjee, P.S., Reynoso-Robles, R., Pérez-Guillé, B., Gayosso-Chávez, C., Torres-Jardón, R., Cross, J.V., Ahmed, I.A.M., Karloukovski, V.V., Maher, B.A., 2019. Combustion- and friction-derived magnetic air pollution nanoparticles in human hearts. Environ. Res. 176, 108567. https://doi.org/10.1016/j.envres.2019.108567.

Castañeda-Miranda, A.G., Chaparro, M.A.E., Chaparro, M.A.E., Böhnel, H.N., 2016. Magnetic properties of *Tillandsia recurvata* L. and its use for biomonitoring a Mexican metropolitan area. Ecol. Indic. 60, 125-136. http://dx.doi.org/10.1016/j.ecolind.2015.06.025.

Castañeda-Miranda, A.G., Chaparro, M.A.E., Marié, D.C., Chaparro, M.A.E., 2018. Uso de la epífita *Tillandsia recurvata* para biomonitoreo magnético de contaminación atmosférica en La Plata, Argentina [Use of *Tillandsia recurvata* for magnetic biomonitoring of atmospheric pollution in La Plata, Argentina]. Geos 38(1), 79-80.

Castañeda-Miranda, A.G., Chaparro, M.A.E., Pacheco-Castro, A., Chaparro, M.A.E., Böhnel, H.N., 2020. Magnetic biomonitoring of atmospheric dust using tree leaves of *Ficus benjamina* in Querétaro (México). Environ. Monit. Assessment. 192, 382. https://doi.org/10.1007/s10661-020-8238-x.

Catinon, M., Ayrault, S., Daudin, L., Sevin, L., Asta, J., Tissut, M., Ravanel, P., 2008. Atmospheric inorganic contaminants and their distribution inside stem tissues of *Fraxinus excelsior* L. Atmos Environ 42 (6), 1223-1238. https://doi.org/10.1016/j.atmosenv.2007.10.082.

Catinon, M., Ayrault, S., Spadini, L., Boudouma, O., Asta, J., Tissut, M., Ravanel, P., 2011. Tree bark suber-included particles: A long-term accumulation site for elements of atmospheric origin. Atmos Environ 45 (5), 1102-1109. https://doi.org/10.1016/j.atmosenv.2010.11.038.

Censo, 2010. Open Data, Municipalidad de General Pueyrredón. https://datos.mardelplata.gob.ar/?q=dataset/censo-2010-poblaci%C3%B3n. https://datos.mardelplata.gob.ar/?q=dataset/fracciones-censales (accessed 19 June 2020)

Chan, D., Stachowiak, G.W., 2004. Review of automotive brake friction materials. Proc. Inst. Mech. Engrs. Part D: J. Automobile Engineering 218(D), 953-966. https://doi.org/10.1243/0954407041856773.

Chaparro, M.A.E., Nuñez, H., Lirio, J.M., Gogorza, C.G.S., Sinito, A.M., 2007. Magnetic screening and heavy metal pollution studies in soils from Marambio station. Antarctic Sci. 19 (3), 379-393. https://doi.org/10.1017/S0954102007000454.

Chaparro, M.A.E., Marié, D.C., Gogorza, C.S.G., Navas, A., Sinito, A.M., 2010. Magnetic studies and scanning electron microscopy X-ray energy dispersive spectroscopy analyses of road sediments, soils, and vehicle-derived emissions. Stud. Geophys. Geod. 54 (4), 633-650. https://doi.org/10.1007/s11200-010-0038-2.

Chaparro, M.A.E., Lavornia, J.M., Chaparro, M.A.E., Sinito, A.M., 2013. Biomonitors of urban air pollution: magnetic studies and SEM observations of corticolous foliose and microfoliose lichens and their suitability for magnetic monitoring. Environ. Pollut. 172, 61–69. https://doi.org/10.1016/j.envpol.2012.08.006.

Ente Municipal de Servicios Urbanos (EMSUR), 2018. Listado de especies recomendadas [List of recommended species]. https://www.mardelplata.gob.ar/documentos/enosur/arboles%20de%20vereda.pdf. Accessed 26 March 2020.

Escalante, J.E., Böhnel, H.N., 2011. Diseño y Construcción de una Balanza de Curie [Design and construction of a Curie Balance]. Geos 31(1), 63.

Fabian, K., Reimann, C., McEnroe, S.A., Willemoes-Wissing, B., 2011. Magnetic properties of terrestrial moss (*Hylocomium splendens*) along a north-south profile crossing the city of Oslo, Norway. Sci. Total Environ. 409(11), 2252-2260. https://doi.org/10.1016/j.scitotenv.2011.02.018.

Flanders, P.J., 1994. Collection, measurement, and analysis of airborne magnetic particulates from pollution in the environment. J. App. Phys. 75 (10), 5931-5936. http://dx.doi.org/10.1063/1.355518.

Gargiulo, J.D.; Kumar, S.R.; Chaparro, M.A.E.; Chaparro, M.A.E.; Natal, M.; Rajkumar, P. Magnetic properties of air suspended particles in thirty eight cities from south India. Atmos. Pollut. Res. 7, 626–637. http://dx.doi.org/10.1016/j.apr.2016.02.008.

Gietl, J.K., Lawrence, R., Thorpe, A.J., Harrison, R.M., 2010. Identification of brake wear particles and derivation of a quantitative tracer for brake dust at a major road. Atmos. Environ. 44 (2), 141-146. https://dx.doi.org/10.1016/j.atmosenv.2009.10.016.

Gómez, Rocío Q., 2019. Biomonitoreo magnético de la contaminación atmosférica en la ciudad de Mar del Plata [Magnetic biomonitoring of the atmospheric pollution in Mar del Plata]. Master of Science Thesis, in Spanish. Universidad Nacional de la Provincia de Buenos Aires, 103 pp. https://www.ridaa.unicen.edu.ar/xmlui/handle/123456789/2010. Accessed 18 March 2020.

Han, X., Naeher, L.P., 2006. A review of traffic-related air pollution exposure assessment studies in the developing world. Environ. Int. 32(1) 106-120. https://doi.org/10.1016/j.envint.2005.05.020.

Huhn, G., Schulz, H., Stärk, H.-J., Tölle, R., Schüürmann, G., 1995. Evaluation of regional heavy metal deposition by multivariate analysis of element contents in pine tree barks. Water Air Soil Pollut 84, 367–383. https://doi.org/10.1007/BF00475349.

I Informe Anual de Mar del Plata: entre todos, monitoreo ciudadano, 2015. https://mardelplataentretodos.org/documentos. Accessed 24 March 2020.

Karagulian, F., Dora, C., Belis, C.A., Dora, C.A.C., Prüss-Ustün, A., Bonjour, S., Adair-Rohani, H., Amann, M., 2015. Contributions to cities' ambient particulate matter (PM): a systematic review of local source contributions at global level. Atm. Environ. 120, 475-483. https://doi.org/10.1016/j.atmosenv.2015.08.087.

King, J., Banerjee, S.K., Marvin, J., Özdemir, Ö., 1982. A comparison of different magnetic methods for determining the relative grain size of magnetite in natural materials: Some results from lake sediments. Earth Planet. Sci. Lett. 59, 404-419. https://doi.org/10.1016/0012-821X(82)90142-X.

Kletetschka, G., Žila, V., Wasilewski, P.J., 2003. Magnetic anomalies on the tree trunks. Stud. Geophys. Geod. 47, 371-379. https://doi.org/10.1023/A:1023779826177.

Knox E.G., 2006. Roads, railways and childhood cancers. J. Epidemiol. Community Health 60, 136-141. https://doi.org/10.1136/jech.2005.042036

Lehndorff, E., Urbat, M., Schwark, L., 2006. Accumulation histories of magnetic particles on pine needles as function of air quality. Atmos. Environ. https://doi.org/10.1016/j.atmos env.2006.06.008

Lim, M.C.H., Ayodo, G.A., Morawska, L., Ristovski, Z.D., Jayaratne, E.R., 2007. The effects of fuel characteristics and engine operating conditions on the elemental composition of emissions from duty diesel buses. Fuel 86, 1831-1839. https://doi.org/10.1016/j.fuel.2006.11.025.

Lin, C.-C., Chen, S.-J., Huang, K.L., 2005. Characteristics of metals in nano/ultrafine/fine/coarse particles collected beside a heavily trafficked road. Environ. Sci. Technol. 39, 8113-8122. https://doi.org/10.1021/es048182a.

Lu, S.-G., Bai, S.-Q., Cai, J.-B., Xu, C., 2005. Magnetic properties and heavy metal contents of automobile emission particulates. J. Zhejiang Univ. Sci. 6B(8), 731-735. https://doi.org/10.1631/jzus.2005.B0731

Liu, Q., Roberts, A.P., Larrasoaña, J.C., Banerjee, S.K., Guyodo, J., Tauxe, L., Oldfield, F., 2012. Environmental magnetism: Principles and applications. Rev. Geophys. 50, RG4002. https://doi.org/10.1029/2012RG000393.

Maher, B.A., Moore, C., Matzka J., 2008. Spatial variation in vehicle-derived metal pollution identified by magnetic and elemental analysis of roadside tree leaves. Atmos. Environ. 42, 364-373. https://doi.org/10.1016/j.atmosenv.2007.09.013.

Maher, B.A., 2019. Airborne magnetite- and iron-rich pollution nanoparticles: Potential neurotoxicants and environmental risk factors for neurodegenerative disease, including Alzheimer's disease. J. Alzheimer's Disease, 1-14. https://doi.org/10.3233/jad-190204.

Maher, B.A.; Ahmed, I.A.M.; Karloukovski, V.; MacLaren, D.A.; Foulds, P.G.; Allsop, D.; Mann, D.M.A.; Torres-Jardón, R.; Calderon-Garciduenas, L., 2016. Magnetite pollution nanoparticles in the human brain. Proc. Natl. Acad. Sci. USA 113, 10797-10801. https://doi.org/10.1073/pnas.1605941113.

Marié, D.C., Chaparro, M.A.E, Irurzun, M.A., Lavornia, J.M., Marinelli, C., Cepeda, R., Böhnel, H.N., Castañeda-Miranda, A.G., Sinito, A.M., 2016. Magnetic mapping of air pollution in Tandil city (Argentina) using the lichen *Parmotrema pilosum* as biomonitor. Atmos. Pollut. Res. 7, 513-520. https://doi.org/10.1016/j.apr.2015.12.005

Marié, D.C., Chaparro, M.A.E., Lavornia, J.M., Sinito, A.M., Castañeda-Miranda, A.G., Gargiulo, J.D., Chaparro, M.A.E., Böhnel, H.N., 2018. Atmospheric pollution assessed by in situ measurement of magnetic susceptibility on lichens. Ecol. Indic. 95, 831-840. https://doi.org/10.1016/j.ecolind.2018.08.029.

Matzka, J., Maher, B.A., 1999. Magnetic biomonitoring of roadside tree leaves: identification of spatial and temporal variations in vehicle-derived particulates. Atm. Environ. 33, 4565–4569. https://doi.org/10.1016/S1352-2310(99)00229-0.

McIntosh, G., Gómez-Paccard, M., Osete, M. L., 2007. The magnetic properties of particles deposited on *Platanus x hispanica* leaves in Madrid, Spain, and their temporal and spatial variations. Sci. Total Environ. 382(1), 135–146. https://10.1016/j.scitotenv.2007.03.020.

Mejía-Echeverry, D., Chaparro, M.A.E., Duque-Trujillo, J.F., Chaparro, M.A.E., Castañeda-Miranda, A.G., 2018. Magnetic biomonitoring of air pollution in a tropical valley using a *Tillandsia* sp. Atmosphere 9, 283. https://doi.org/10.3390/atmos9070000.

Moreno, E., Sagnotti, L., Dinares-Turell, J., Winkler, A., Cascella, A., 2003. Biomonitoring of traffic air pollution in Rome using magnetic properties of tree leaves. Atmos. Environ. 37, 2967-2977. https://doi.org/10.1016/S1352-2310(03)00244-9.

Palmgren, F., Waahlin, P., Kildesó, J., Afshari, A., Fogh, C.L., 2003. Characterisation of particle emissions from the driving car fleet and the contribution to ambient and indoor particle concentrations. Phys. Chem. Earth 28, 327-334. https://doi.org/10.1016/S1474-7065(03)00053-6.

Paoli, L., Winkler, A., Guttová, A., Sagnotti, A., Grassi, A., Lackovičová, A., Senko, D., Loppi, S., 2017. Magnetic properties and element concentrations in lichens exposed to airborne pollutants released during cement production. Environ. Sci. Pollut. Res. 24 (13), 12063-12080. https://doi.org/10.1007/s11356-016-6203-6.

Pope, C.A., Dockery, D.W., 2006. Health effects of fine particulate air pollution: lines that connect. J. Air Waste Manage. Assoc. 56, 709-742. https://doi.org/10.1080/10473289.2006.10464485

Rai, P.K., 2013. Environmental magnetic studies of particulates with special reference to biomagnetic monitoring using roadside plant leaves. Atmos. Environ. 72, 113-129. https://doi.org/10.1016/j.atmosenv.2013.02.041.

Sagnotti, L., Taddeucci, J., Winkler, A., Cavallo, A., 2009. Compositional, morphological, and hysteresis characterization of magnetic airborne particulate matter in Rome, Italy, Geochem. Geophys. Geosyst. 10, Q08Z06. https://doi.org/10.1029/2009GC002563.

Tomlinson, D.L., Wilson, J.G., Harris, C.R., Jeffrey, D.W., 1980. Problems in the assessment of heavy metals levels in estuaries and the formation of a pollution index. Helgol Meeresunters 33, 566-575. https://doi.org/10.1007/BF02414780.

Vuković, G., Aničić Urošević, M., Tomašević, M., Samson, R., Popović, A., 2015. Biomagnetic monitoring of urban air pollution using moss bags (*Sphagnum girgensohnii*). Ecol. Indic. 52, 40-47. https://doi.org/10.1016/j.ecolind.2014.11.018.

Salo, H., Paturi, P., Mäkinen, J., 2016. Moss bag (*Sphagnum papillosum*) magnetic and elemental properties for characterizing seasonal and spatial variation in urban pollution. Int. J. Environ. Sci. Technol. 13 (6), 1515-1524. https://doi.org/10.1007/s13762-016-0998-z.

Salo, H., Mäkinen, J., 2019. Comparison of traditional moss bags and synthetic fabric bags in magnetic monitoring of urban air pollution. Ecol. Indic. 104, 559-566. https://doi.org/10.1016/j.ecolind.2019.05.033.

Sanders, P., Xu, N., Dalka, T., Maricq, M.M., 2003. Airborne brake wear debris: Size distributions, composition, and a comparison of dynamometer and vehicle test, Environ. Sci. Technol. 37, 4060–4069. https://doi.org/10.1021/es034145s.

Vezzola, L.C., Muttoni, G., Merlini, M., Rotiroti, N., Pagliardini, L., Hirt, A.M., Pelfini, M., 2017. Investigating distribution patterns of airborne magnetic grains trapped in tree barks in Milan, Italy: insights for pollution mitigation strategies, Geophysical Journal International 210 (2), 989–1000. https://doi.org/10.1093/gji/ggx232.

Winkler, A., Caricchi, C., Guidotti, M., Owczarek, M., Macri, P., Nazzari, M., Amoroso, A., Di Giosa, A., Listrani, S., 2019. Combined magnetic, chemical and morphoscopic analyses on lichens from a complex anthropic context in Rome, Italy. Sci. Total Environ. 690, 1355-1368. https://doi.org/10.1016/j.scitotenv.2019.06.526.

Winkler, A., Contardo, T., Vannini, A., Sorbo, S., Basile, A., Loppi, S., 2020. Magnetic emissions from brake wear are the major source of airborne particulate matter bioaccumulated by lichens exposed in Milan (Italy). App. Sci. 10, 2073. https://doi.org/10.3390/app10062073.

Walden, J., Oldfield, F., Smith, J.P. (Eds.), 1999. Environmental Magnetism: a practical guide. Technical Guide, No. 6. Quaternary Research Association, London (243 pp).

Weckwerth, G., 2001. Verification of traffic emitted aerosol components in the ambient air of Cologne (Germany). Atmos. Environ. 35, 5525-5536. https://doi.org/10.1016/S1352-2310(01)00234-5.

Zhang, C.X., Huang, B.C., Piper, J.D.A., Luo, R.S., 2008. Biomonitoring of atmospheric particulate matter using magnetic properties of *Salix matsudana* tree ring cores. Sci. Total Environ. 393, 177-190. https://doi.org/10.1016/j.scitotenv.2007.12.032.

Table and Figure captions

Table 1. Descriptive statistics of magnetic parameters and potentially toxic elements. Street tree bark samples (MC - samples) from Mar del Plata collected in April 2016.

Fig. 1. Study area (Mar del Plata, Argentina) and collection/in situ measurement sites.

Fig. 2. Studied street tree species in the urbanized area (Mar del Plata downtown). A total of 54 trees were identified and studied.

Fig. 3. Magnetic measurements of street tree bark samples: (**a**) thermomagnetic measurements; and (**b**) saturation of isothermal remanent magnetization versus mass specific magnetic susceptibility.

Fig. 4. SEM-EDS analysis of micron and sub-micron Fe oxides trapped by street tree barks: (**a**, **c**, **e**) sample MC-3.4, and (**b**, **d**, **f**) sample MC-3.7.

Fig. 5. Magnetic particles trapped by street tree barks from Mar del Plata, sizes are estimated from (**a**) parameters χ_{ARM} and χ (calibration lines are based on data reported by King et al., 1982) and (**b**) the anhysteretic ratio χ_{ARM}/χ. For comparison purposes, reported data (and mean values ± s.d.) using lichen sp. in Tandil (170 km NW from the studied area, Marié et al., 2016) and Mar del Plata (Gómez, 2019), Tillandsia sp. in La Plata (340 km N from the studied area, Castañeda-Miranda et al., 2018), and traffic derived particles (Marié et al., 2010) are shown.

Fig. 6. Prediction maps using measurements of the magnetic proxy for air pollution: mass specific susceptibility χ in 10^{-8} m^3 kg^{-1} (**a**) April 2016; (**b**) March 2017.

Fig. 7. (**a**) Prediction map using measurements of the magnetic proxy for air pollution: in situ magnetic susceptibility κ_{is} in 10^{-5} SI (March 2017), and (**b**) recorded traffic and population density (data provided by Censo, 2010).

Table 1

Variable	N	mean	s.d.	min.	max.
χ [10^{-8} m^3 kg^{-1}]	54	82.2	40.0	18.4	218
SIRM [10^{-3} Am^2 kg^{-1}]	54	9.3	4.3	2.5	19.2
χ_{ARM} [10^{-8} m^3 kg^{-1}]	54	287	139	87.9	689
χ_{fd}% [%]	54	4.1	3.8	-0.8	16.9
χ_{ARM}/χ [a.u.]	54	4.0	2.4	1.8	18.4
ARM/SIRM [a.u.]	54	0.03	0.01	0.01	0.07
SIRM/χ [kA/m]	54	13.1	8.4	4.9	53.0
H_{cr} [mT]	54	37.0	2.4	27.0	40.2
S-ratio [a.u.]	54	--	--	0.80	1
Ba [mg kg^{-1}]	27	101	40	27	186
Co [mg kg^{-1}]	27	0.9	0.9	0.1	3.2
Cr [mg kg^{-1}]	27	4.8	2.7	1.0	12.3
Cu [mg kg^{-1}]	27	48	22	18	95
Fe [mg kg^{-1}]	27	3160	1560	1230	6820
Mo [mg kg^{-1}]	27	1.07	0.39	0.56	2.04
Ni [mg kg^{-1}]	27	2.9	1.0	1.1	4.6
Pb [mg kg^{-1}]	27	32.4	24.1	6.0	109
Sb [mg kg^{-1}]	27	2.5	2.1	0.5	9.9
Sn [mg kg^{-1}]	27	1.4	0.7	0.3	3.0
V [mg kg^{-1}]	27	5.4	2.2	2.5	11.3
Zn [mg kg^{-1}]	27	1650	766	587	3530
PLI [a.u.]	27	3.3	1.3	1.2	6.2

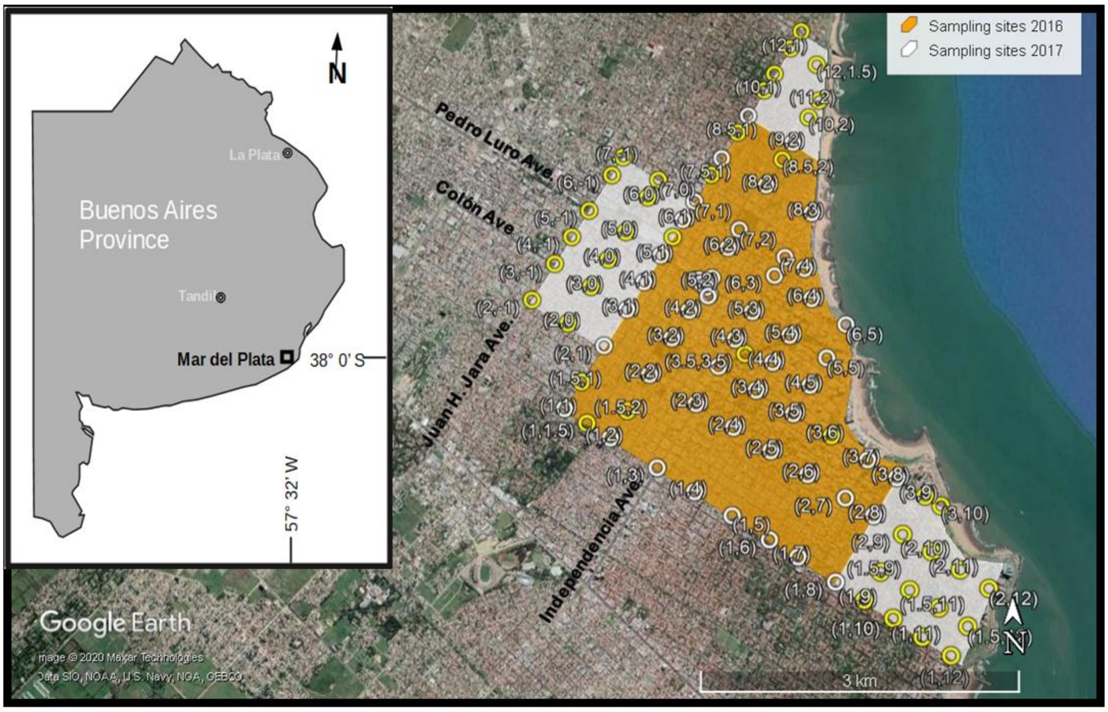
Sampling sites 2016
Sampling sites 2017
N
La Plata
Buenos Aires Province
Tandil
Mar del Plata
38° 0' S
57° 32' W
Pedro Luro Ave.
Colón Ave.
Juan H. Jara Ave.
Independencia Ave.
Google Earth
3 km

Figure 1

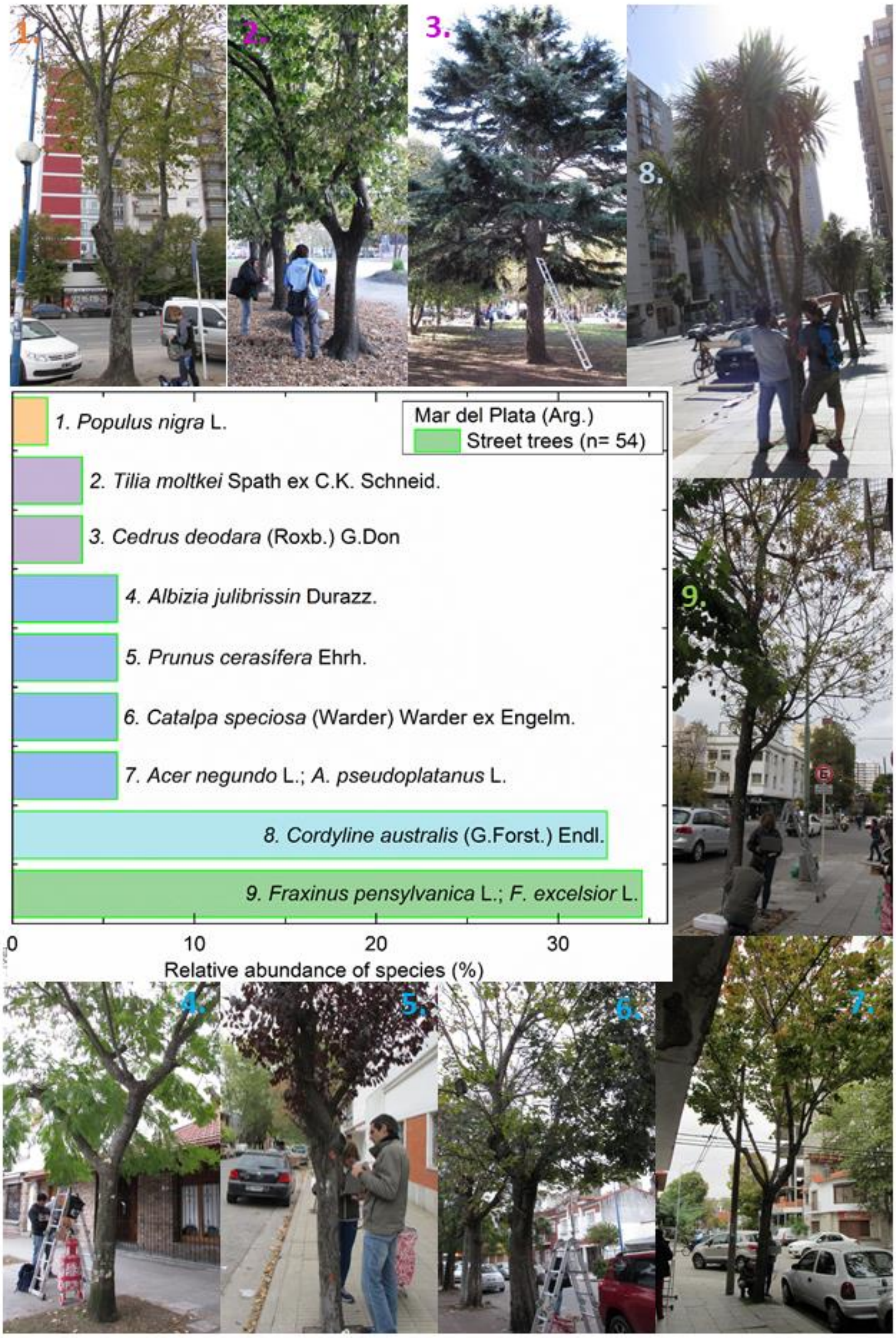
1.
2.
3.
8.
9.
4.
5.
6.
7.
1. Populus nigra L.
2. Tilia moltkei Spath ex C.K. Schneid.
3. Cedrus deodara (Roxb.) G.Don
4. Albizia julibrissin Durazz.
5. Prunus cerasifera Ehrh.
6. Catalpa speciosa (Warder) Warder ex Engelm.
7. Acer negundo L.; A. pseudoplatanus L.
8. Cordyline australis (G.Forst.) Endl.
9. Fraxinus pensylvanica L.; F. excelsior L.
Mar del Plata (Arg.)
Street trees (n= 54)
0
10
20
30
Relative abundance of species (%)

Figure 2

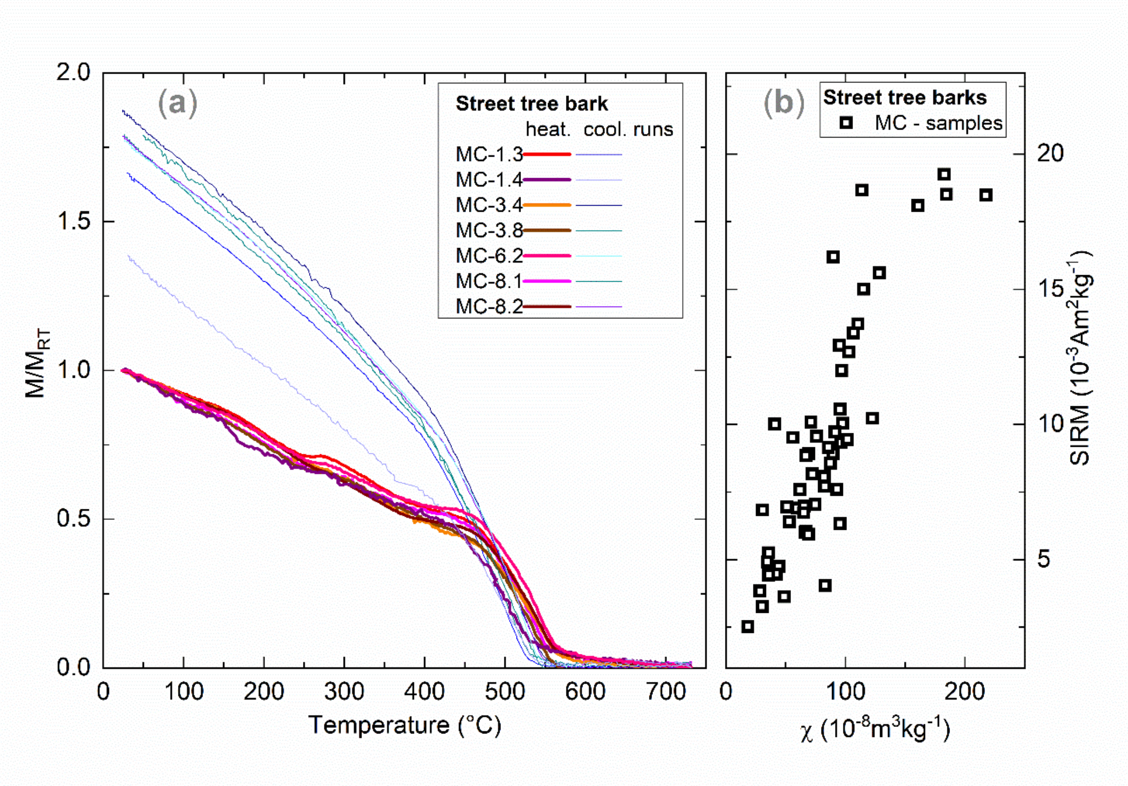

(a)
Street tree bark
heat. cool. runs
MC-1.3
MC-1.4
MC-3.4
MC-3.8
MC-6.2
MC-8.1
MC-8.2
M/M_RT
Temperature (°C)
(b)
Street tree barks
MC - samples
SIRM (10^-3Am^2kg^-1)
χ (10^-8m^3kg^-1)

Figure 3

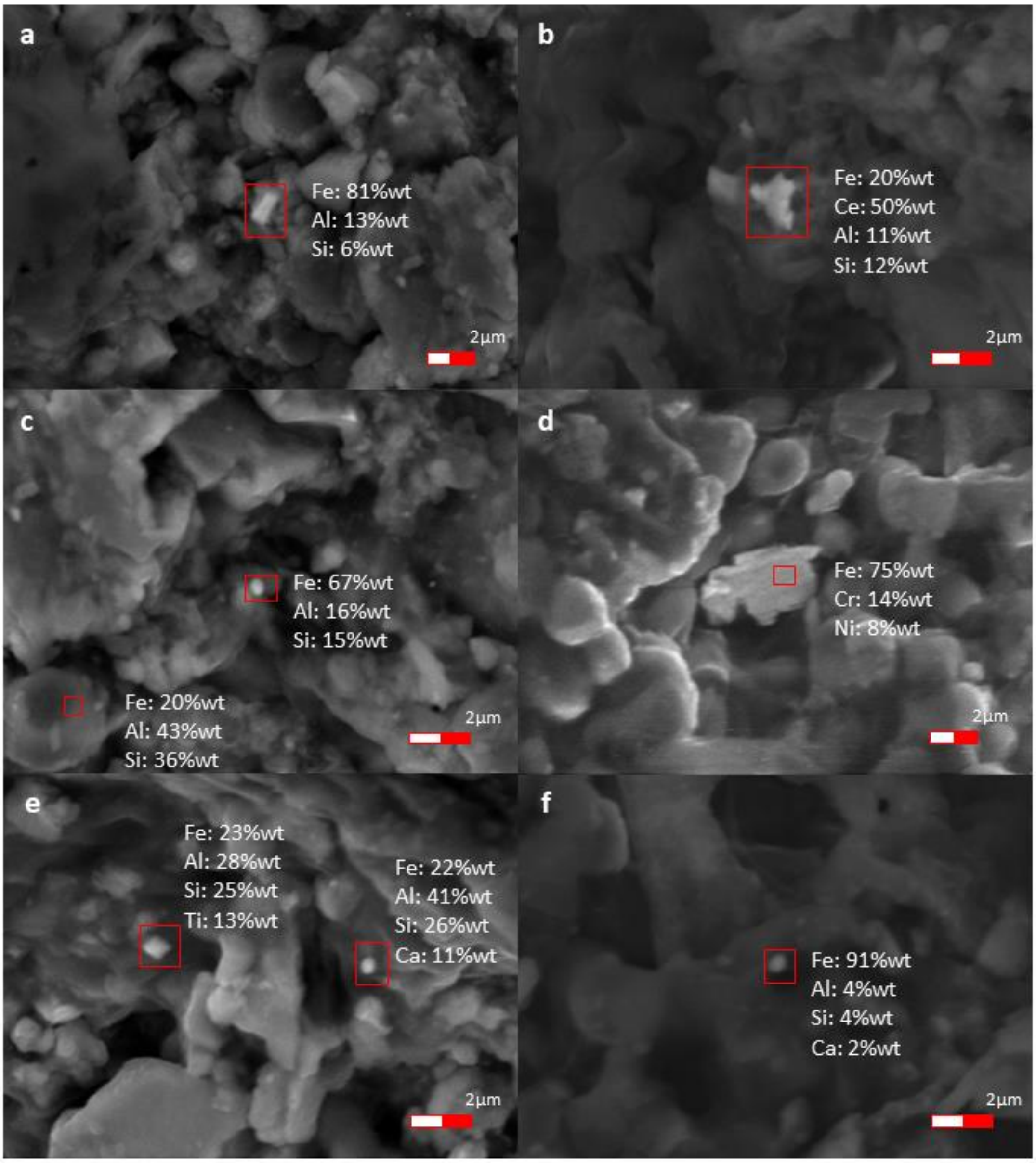
a
Fe: 81%wt
Al: 13%wt
Si: 6%wt
2μm
b
Fe: 20%wt
Ce: 50%wt
Al: 11%wt
Si: 12%wt
2μm
c
Fe: 67%wt
Al: 16%wt
Si: 15%wt
Fe: 20%wt
Al: 43%wt
Si: 36%wt
2μm
d
Fe: 75%wt
Cr: 14%wt
Ni: 8%wt
2μm
e
Fe: 23%wt
Al: 28%wt
Si: 25%wt
Ti: 13%wt
Fe: 22%wt
Al: 41%wt
Si: 26%wt
Ca: 11%wt
2μm
f
Fe: 91%wt
Al: 4%wt
Si: 4%wt
Ca: 2%wt
2μm

Figure 4

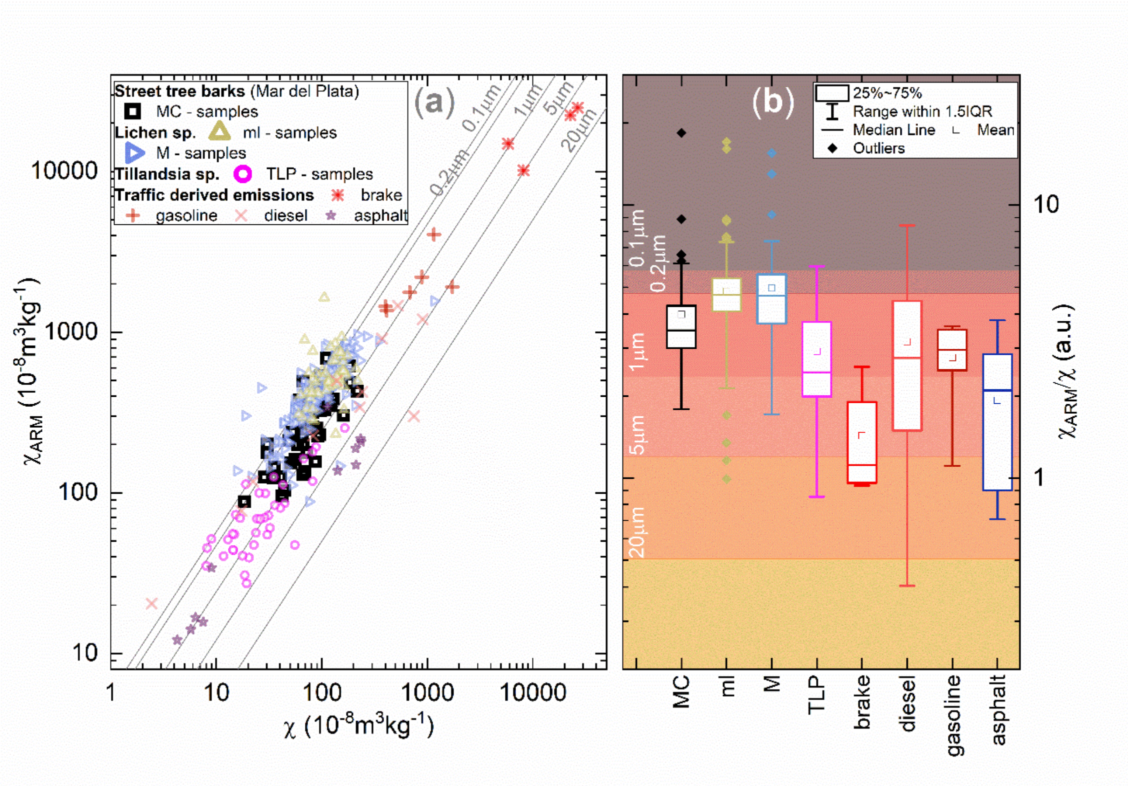

Street tree barks (Mar del Plata)
MC - samples
Lichen sp.
ml - samples
M - samples
Tillandsia sp.
TLP - samples
Traffic derived emissions
brake
gasoline
diesel
asphalt
(a)
0.1µm
0.2µm
1µm
5µm
20µm
χARM (10-8m3kg-1)
χ (10-8m3kg-1)
(b)
25%~75%
Range within 1.5IQR
Median Line
Mean
Outliers
χARM/χ (a.u.)
MC
ml
M
TLP
brake
diesel
gasoline
asphalt

Figure 5

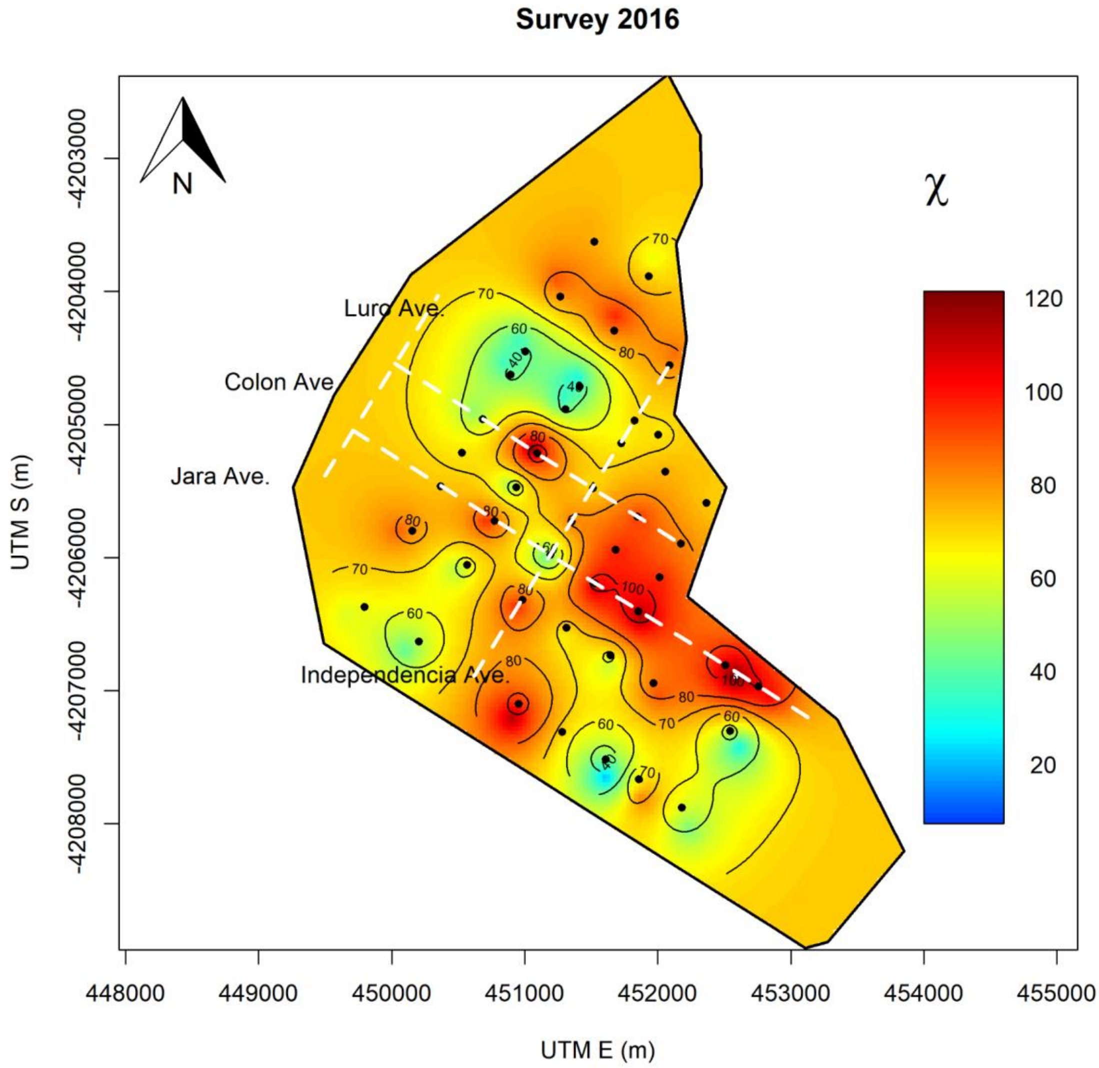

Survey 2016
N
χ
120
100
80
60
40
20
Luro Ave.
Colon Ave.
Jara Ave.
Independencia Ave.
-4203000
-4204000
-4205000
-4206000
-4207000
-4208000
UTM S (m)
448000
449000
450000
451000
452000
453000
454000
455000
UTM E (m)

Figure 6a

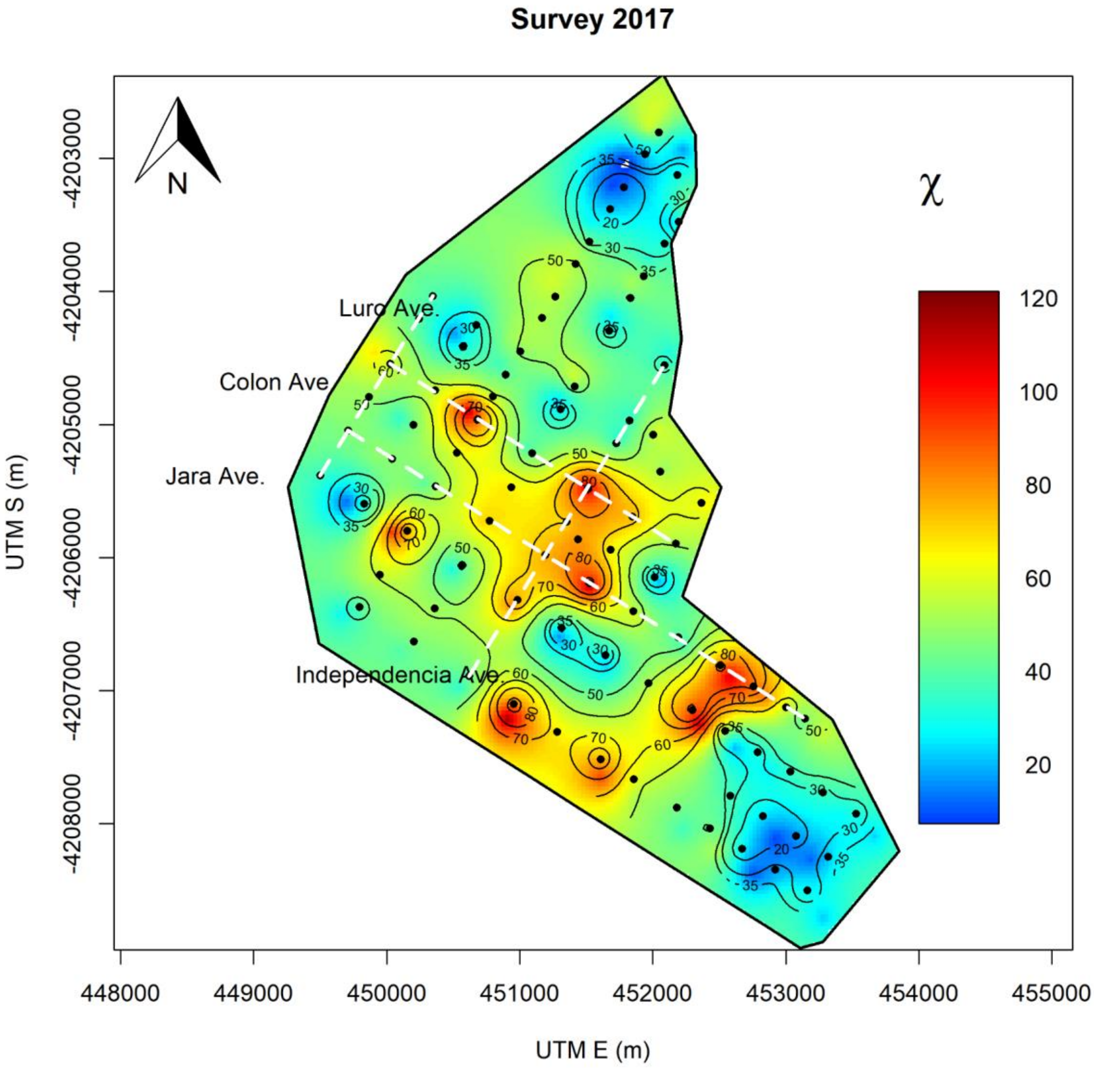
Survey 2017
N
χ
Luro Ave.
Colon Ave.
Jara Ave.
Independencia Ave.
120
100
80
60
40
20
-4203000
-4204000
-4205000
-4206000
-4207000
-4208000
UTM S (m)
448000
449000
450000
451000
452000
453000
454000
455000
UTM E (m)

Figure 6b

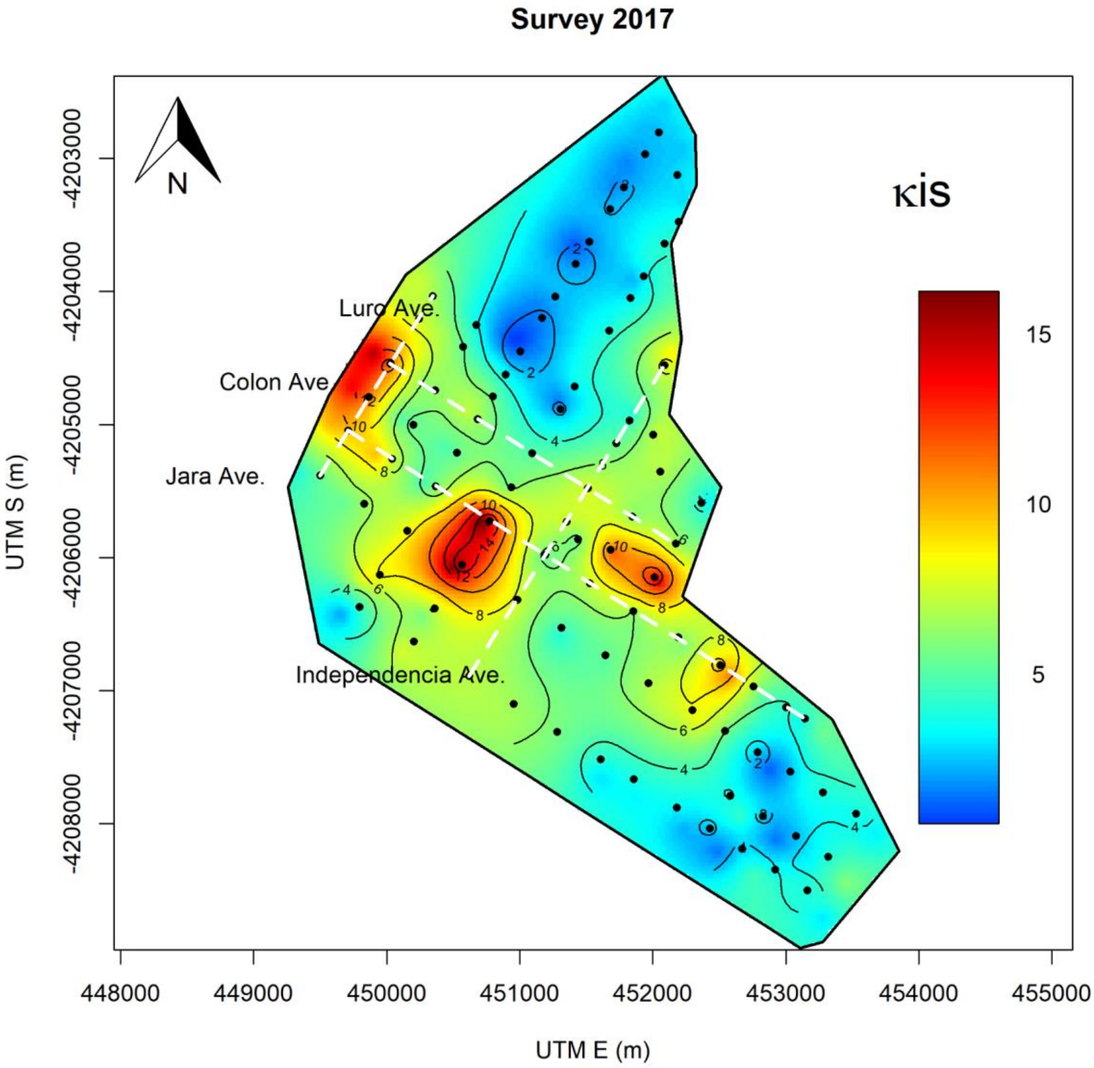
Survey 2017
N
κis
15
10
5
Luro Ave.
Colon Ave.
Jara Ave.
Independencia Ave.
UTM S (m)
-4203000
-4204000
-4205000
-4206000
-4207000
-4208000
448000
449000
450000
451000
452000
453000
454000
455000
UTM E (m)

Figure 7a

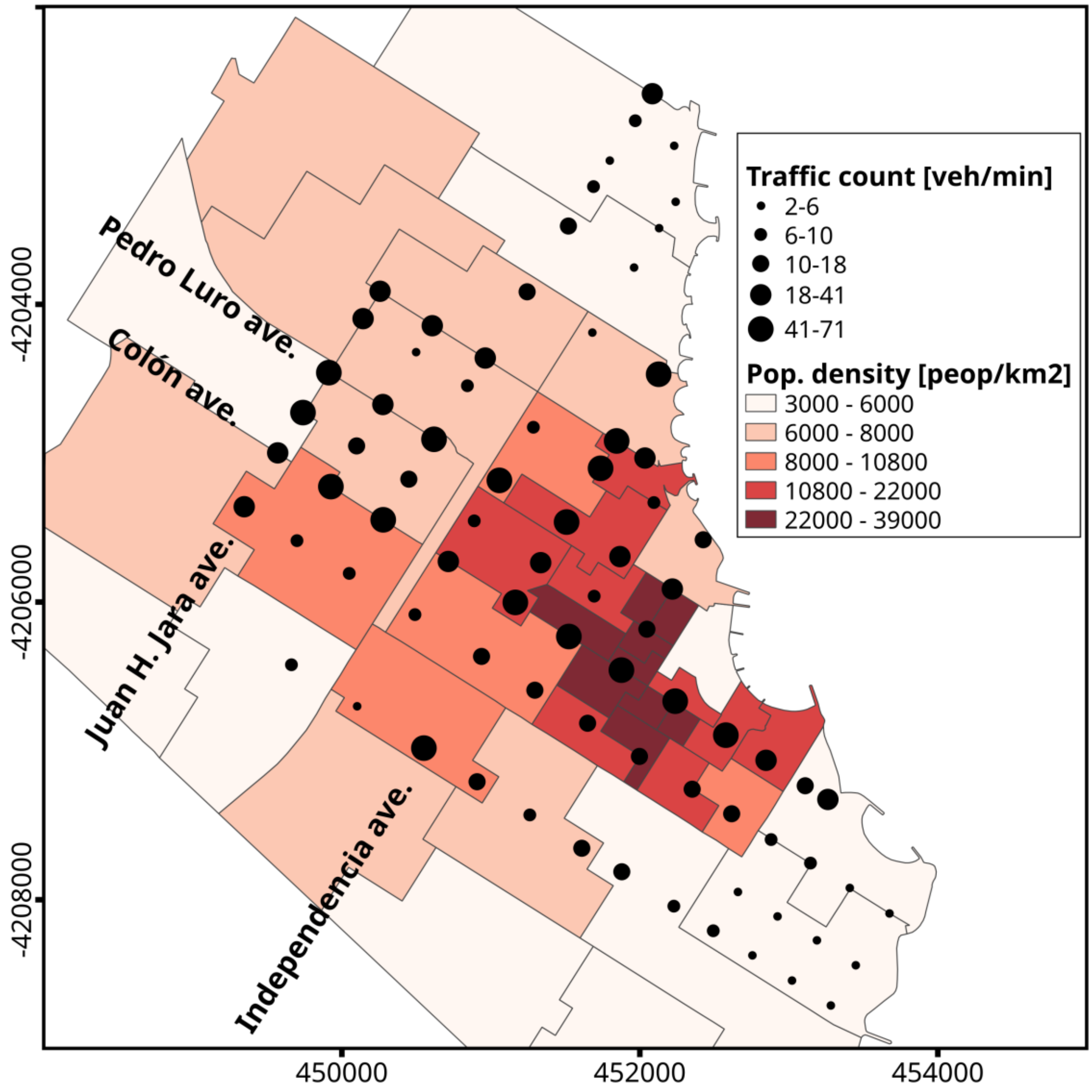
Traffic count [veh/min]
2-6
6-10
10-18
18-41
41-71
Pop. density [peop/km2]
3000 - 6000
6000 - 8000
8000 - 10800
10800 - 22000
22000 - 39000
Pedro Luro ave.
Colón ave.
Juan H. Jara ave.
Independencia ave.
-4204000
-4206000
-4208000
450000
452000
454000

Figure 7b

Highlights

Accumulated airborne magnetic particles are inhalable $PM_{2.5}$ and potentially harmful

In situ magnetic biomonitoring is rapid and convenient for air PM pollution assessment

Street tree barks are an efficient option for particle biomonitoring